

Phase Separation within a Binary Self-Assembled Monolayer on Au{111} Driven by an Amide-Containing Alkanethiol

Rachel K. Smith,[†] Scott M. Reed,[‡] Penelope A. Lewis,[†] Jason D. Monnell,[†] Robert S. Clegg,^{‡,§} Kevin F. Kelly,[†] Lloyd A. Bumm,[†] James E. Hutchison,^{*,‡} and Paul S. Weiss^{*,†}

Department of Chemistry, The Pennsylvania State University, University Park, Pennsylvania 16802-6300, and Department of Chemistry and Materials Science Institute, University of Oregon, Eugene, Oregon 97403-1253

Received: September 28, 2000; In Final Form: December 8, 2000

We report the phase separation of a self-assembled monolayer formed from a binary mixture of adsorbates, *n*-decanethiol, and an amide-containing alkanethiol of similar length (3-mercapto-*N*-nonylpropionamide), as studied by scanning tunneling microscopy. While mixtures of *n*-alkanethiols of similar length (i.e., *n*-decanethiol and *n*-dodecanethiol) show no phase separation, the introduction of a hydrogen-bonding functionality buried deep within the film induces the formation of single-component domains on the nanometer scale. Phase separation occurs at all relative compositions studied, and for these molecules maintains the same exposed terminal functionality across the entire film. In nonequimolar concentrations of adsorbates, we observe that the solution component present in greater concentration will dominate the composition of the adsorbed monolayer in super proportion to that in solution, consistent with enthalpic contributions from both the solvent and intermolecular interactions of adsorbates.

While self-assembled monolayers (SAMs) have been proposed for uses in diverse applications,¹ few methods of generating and stabilizing molecular-scale patterns have been demonstrated.² Recent studies have shown evidence of directed assembly and patterning of binary mixtures of adsorbed alkanethiols, either by partial thermal desorption or selective electrochemical desorption with subsequent deposition of a new adsorbate.^{2d,f,j} Surprisingly, only a few examples of nanometer-scale phase separation of such binary mixtures of similar adsorbates are known in SAMs,³ and spontaneous phase separation of binary mixtures of methyl-terminated *n*-alkanethiols of similar length has never been observed.^{2d} Spontaneous phase separation has been observed for ω -functionalized *n*-alkanethiols, where the driving force for separation is the ω -functional group interaction.³ Here we demonstrate phase separation driven by intermolecular interactions buried within the film, showing that it is possible to induce phase separation of SAM components by methods that do not change the general reactivity of the molecular film surface. The strategy demonstrated here provides additional tools for the design of nanostructured monolayer assemblies. Our objective is to control and to manipulate the molecular-scale structures of SAMs en route to the rational design of new and functional devices.

Here we report a scanning tunneling microscope (STM) study on the molecular-scale phase separation of an *internally*-functionalized, amide-containing alkanethiol (3-mercapto-*N*-nonylpropionamide, henceforth **1ATC9**) from an *n*-alkanethiol (*n*-decanethiol) on Au{111} under ambient conditions *without* post-assembly treatment. We hypothesize that intermolecular hydrogen bonding of the buried amide functionality (see Figure

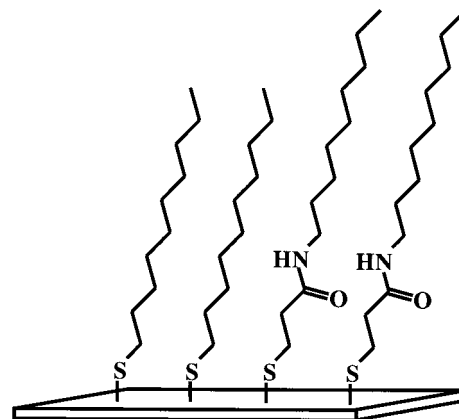


Figure 1. Schematic of **1ATC9** (right) and *n*-decanethiolate (left) coadsorbed on a Au{111} substrate.

1) is the primary driving force for the spontaneous formation of nanometer-scale, phase-separated domains upon coadsorption. The long-range structures of the films described here are most likely kinetically trapped rather than equilibrium structures (typical of SAMs in general), yet the observed short-range structure is due to thermodynamic interactions between species adsorbed on the surface. As in our previous work, these STM images are single snapshots of the structures obtained.^{3a} The formation of phase-separated domains is indicative of adsorbate assemblies and conformations that are both energetically favorable and accessible at ambient temperature.^{3a} SAMs that preferentially self-assemble into discrete domains are of marked importance in the future design of nanoscale structures.

Mixed monolayers were prepared by coadsorption from solutions of **1ATC9** and *n*-decanethiol in N₂-sparged, absolute ethanol onto flame-annealed, mica-supported gold substrates (deposition solutions were always 1 mM in total thiol).⁴ 3-Mercapto-*N*-nonylpropionamide was prepared by previously described methods.⁵ Substrates were typically exposed to thiol

* To whom correspondence should be addressed: (JEH) hutch@oregon.uoregon.edu; (PSW) stm@psu.edu.

[†] The Pennsylvania State University.

[‡] University of Oregon.

[§] Current address: Noyes Laboratory of Chemical Physics, California Institute of Technology, Pasadena, California, 91125.

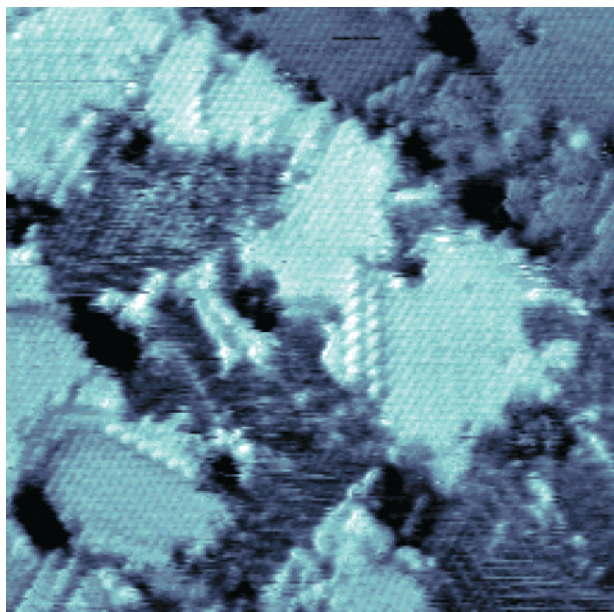


Figure 2. STM image of a $300 \text{ \AA} \times 300 \text{ \AA}$ area of a phase-separated SAM formed by coadsorption from an equimolar solution of **1ATC9** and *n*-decanethiol (1mM in total thiol). The image was recorded at a sample bias of +1.0 V and a tunneling current of 1.0 pA. Topographically higher regions correspond to the brighter areas.

solution for 40 h, after which they were rinsed with absolute ethanol and blown dry with N_2 . All STM experiments were performed under ambient conditions using a home-built STM as described previously.^{2d} Images were typically recorded with a sample bias of +1.0 V, and tunneling currents of either 1.0 or 2.0 pA.

Well-ordered, phase-separated domains of both the **1ATC9** and *n*-decanethiolate species on the gold terraces are resolved on the molecular scale (Figure 2). The two adsorbates are similar in length, with **1ATC9** being only three backbone atoms longer, containing one additional methylene and an amide group. The amide-containing molecules correspond to the topographically higher (displayed as brighter) regions in the image (confirmed by studies in which the relative concentrations of the components were varied); the rows of protrusions within some of the **1ATC9** regions are characteristic of STM images of molecules at specific types of structural domain boundaries (as commonly observed for *n*-alkanethiolate monolayers).⁶ The measured STM topographic height difference between the molecules is roughly 1.5 Å (about half of the physical height difference), consistent with our understanding of the convolution between physical and electronic properties of these molecular films when imaged by STM.⁷ In Figure 2, a monatomic gold step runs through the upper right-hand corner (2.4 Å in height), creating what might otherwise appear to be two separate domains of differing adsorbates; the Au substrate steps may be seen more clearly in an image of larger area (Figure 3). Grain boundaries and vacancy islands in the gold substrate (typically seen in STM images of SAMs prepared at room temperature) are visible. Substrate vacancies can be distinguished from the adsorbate domains as they tend to be (roughly) circular in shape and of a characteristic height (one gold atom deep).

Phase separation of these molecules is also found in SAMs for which the deposition solutions are not equimolar in the two adsorbates. Figure 4 is an STM image of a monolayer formed by exposing a gold substrate to an adsorbate solution composed of a 1:3 mole ratio of **1ATC9** and *n*-decanethiol (1 mM in total thiol). The **1ATC9** adsorbates are visible on the surface, but

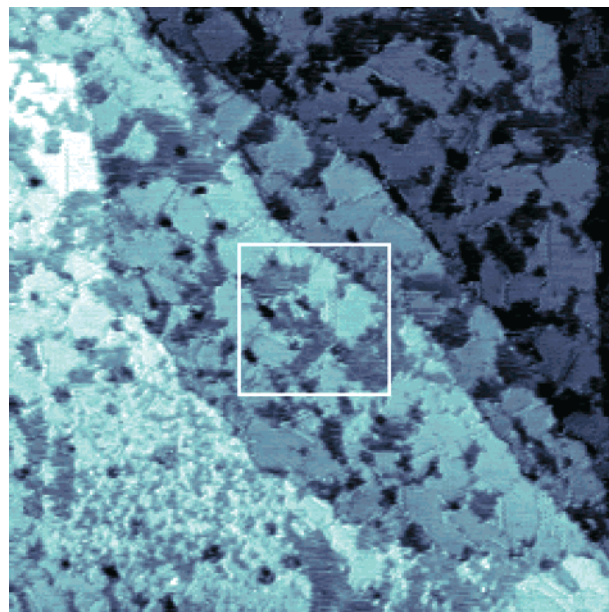


Figure 3. STM image of a $1200 \text{ \AA} \times 1200 \text{ \AA}$ area of a phase-separated SAM formed by coadsorption from an equimolar solution of **1ATC9** and *n*-decanethiol (1mM in total thiol). The image was recorded at a sample bias of +1.0 V and a tunneling current of 1.0 pA. The white box corresponds to the area imaged in Figure 2.

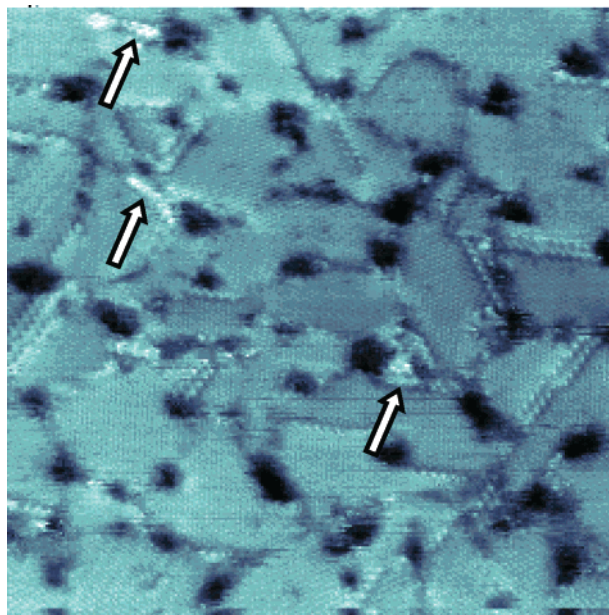


Figure 4. STM image of a $580 \text{ \AA} \times 580 \text{ \AA}$ area of a monolayer formed from a 1:3 mole ratio (adsorption solution) of **1ATC9** and *n*-decanethiol. The image was recorded at a sample bias of +1.0 V and a tunneling current of 2.0 pA. The arrows point to areas of **1ATC9** adsorption in the *n*-decanethiolate matrix.

are present in significantly lower concentration (as compared to the corresponding deposition solution). In both this figure and images for even lower **1ATC9** concentrations, the **1ATC9** molecules bind to the surface at the edge of these vacancies and at grain boundaries in the *n*-decanethiolate matrix. The most likely reason for such directed nucleation of the **1ATC9** molecules in the SAM is that it would be energetically unfavorable for the polar amide moiety to be buried within the crystalline matrix of the apolar *n*-decanethiol molecules; therefore, adsorption may occur at sites of minimal van der Waals contact from the surrounding molecules, and also at sites where there may be additional contact with the weakly hydrogen

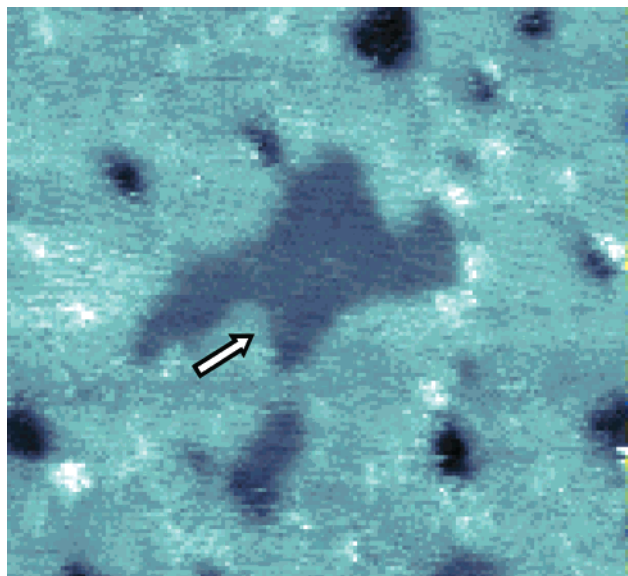


Figure 5. STM image of a $515 \text{ \AA} \times 475 \text{ \AA}$ area of a monolayer formed from a 3:1 mole ratio adsorption solution of **1ATC9** and *n*-decanethiol. The image was recorded at a sample bias of +1.0 V and a tunneling current of 1.0 pA. The arrow points to areas of *n*-decanethiolate adsorption in the **1ATC9** matrix.

bonding ethanol solvent (see below). Flipping of molecules between adjacent domains observed for alkanethiolate monolayers and flow of substrate steps through these films can also result in isolating included molecules such as the amides at domain boundaries of the alkanethiolate matrix.^{8,9} In the upper left-hand corner of Figure 4, amide-containing molecules are adsorbed at a Au vacancy island (the protruding molecular features, displayed as bright, are the **1ATC9**, indicated by arrows). On the opposite side of the Au vacancy, more *n*-decanethiolate molecules are adsorbed. Two additional amide islands can be seen within the image located around surface defects (also indicated by arrows). In monolayers formed from an adsorbate solution of a 1:3 mole ratio of *n*-decanethiol and **1ATC9** (Figure 5), the relative surface coverages are not mirror images of each other (vide infra).

The observed phase segregation in the SAM is presumably the result of enthalpic contributions, as entropy will favor mixing of the constituents within the monolayer. Hydrogen bonding driving the spontaneous phase separation is consistent with observed spectroscopic evidence of hydrogen bonding in undiluted monolayers of **1ATC9**⁴ and the expectation that hydrogen bonding in the SAM will be enhanced by the apolar *n*-decanethiol diluent.¹⁰ The enthalpic stabilization due to hydrogen bonding and van der Waals' interactions can be approximated from the heats of sublimation of analogous compounds.¹¹ The enhanced stabilization of the **1ATC9** phase is approximately $[(8.6 \text{ kJ/mol } -\text{CH}_2-) + (33.5 \text{ kJ/mol H-bond})]$, or 42.1 kJ/mol greater than the interactions between the non-hydrogen bonding constituents of the film. By way of comparison, the total enthalpic contribution of the 10 methylene groups in *n*-decanethiol is $\sim 86 \text{ kJ/mol}$ adsorbate vs our estimate of $\sim 128 \text{ kJ/mol}$ for **1ATC9**. Such differing energetics most likely drives the composition of the final SAM to be different than that of the deposition solution. Previous evidence of closely packed films of SAMs composed of pure amide-containing alkanethiol,^{5,12} coupled with our not having yet observed intercomponent diffusion on the limited time scale of our measurements, leads us to expect that the ordered **1ATC9** domains are more stable than the *n*-decanethiolate domains. Substrate-adsorbate exchange or mobility may be highly limited

in the **1ATC9** due to the steric limitations imposed by the domain having to move in a concerted manner.

As can be seen from Figures 4 and 5, if the relative concentrations of adsorbates in the deposition solution are reversed, the relative surface coverages do not parallel the concentration differences. The **1ATC9** molecules are significantly under-represented in the monolayer when present in low concentrations in the deposition solutions (25% mole fraction and lower), and they are over-represented when on the surface in a greater mole fraction relative to the *n*-decanethiolates. However, the domains of the *n*-decanethiolate molecules within the **1ATC9** matrix are larger and irregularly shaped (Figure 5, arrow) as compared to the **1ATC9** domains within the *n*-decanethiolate matrix (Figure 4, arrows). Although in the gas phase the molecules' affinities for the surface [$\Delta H_{\text{ads}}(\text{1ATC9})$ and $\Delta H_{\text{ads}}(n\text{-decanethiol})$] are roughly equal, the enthalpy of solvation of **1ATC9** in ethanol is greater than that for *n*-decanethiol, effecting a more energetically favorable surface adsorption of *n*-decanethiol than **1ATC9**. However, *once on the surface*, the **1ATC9**–**1ATC9** intermolecular interactions predominate. As in our earlier work,^{3a} we infer from the minimized interface length between the different surface components that the cross-interactions between the *n*-decanethiolates and the **1ATC9** molecules is lower than the attraction between like molecules of either type.

Still, the kinetics of monolayer assembly are certainly a factor in determining ultimate surface composition, especially with regard to adsorbate solubility in the deposition solution. At low relative concentrations of **1ATC9**, the solvation energy of **1ATC9** molecules in ethanol may be greater than that required to adsorb to the surface within an apolar matrix. As the **1ATC9** is so well solvated by the ethanol, *n*-decanethiol may adsorb at higher concentrations and/or at a faster rate; the small amount of **1ATC9** adsorption that may occur is located at naturally occurring defects within the SAM, where solvent molecules may still be present, or is later isolated there via film motion. At higher relative concentrations of **1ATC9**, solvent may partially disrupt the nascent monolayer or interfere with hydrogen bonding between adjacent **1ATC9** molecules, allowing an increased opportunity for *n*-decanethiol molecules to chemisorb to the surface. This proposed solvent effect will be tested in upcoming experiments.

These results show great promise for controlling the patterning and structure of thin films by using buried functionalities of adsorbates. SAM formation is a complex interplay between kinetics and thermodynamics; the observation of short-range phase separation is evidence that enthalpic interactions are important in determining film structure. However, we do not know how close these structures are to thermodynamic equilibrium. Further experiments studying the monolayer structures formed as a function of systematically varying adsorption solvents and deposition times will provide us with a larger database to understand the complicated processes of SAM formation. Elucidating the mechanisms that govern phase separation and the intermolecular interactions of adsorbates may ultimately lead to the creation of nanoscale structures that can be configured in a manner analogous to these experiments. Ongoing experiments examine spontaneous domain formation of related adsorbates, study the packing behavior of these assemblies, and measure electron transfer through the amide-containing adsorbate domains.

Acknowledgment. The authors thank NSF (all), ONR (PSU), DARPA (PSU), the Camille and Henry Dreyfus Founda-

tion (J.E.H. is a Camille Dreyfus Teacher Scholar), the Alfred P. Sloan Foundation (J.E.H. is a Sloan Fellow), and a Department of Education GAANN fellowship (S.M.R.).

References and Notes

- (1) For a general overview of SAM applications, refer to: (a) *Thin Films*, Vol. 24; Ulman, A., Ed.; Academic Press: San Diego, 1998. (b) Ulman, A. *Chem. Rev.* **1996**, 96, 1533. (c) Mrksich, M.; Whitesides, G. M. *Annu. Rev. Biophys. Biomol. Struct.* **1996**, 25, 55. (d) Dubois, L. H.; Nuzzo, R. G. *Annu. Rev. Phys. Chem.* **1992**, 43, 437. (e) Liu, J.; Kim, A. Y.; Wang, L. Q.; Palmer, B. J.; Chen, Y. L.; Bruinsma, P.; Bunker, B. C.; Exarhos, G. J.; Graff, G. L.; Rieke, P. C.; Fryxell, G. E.; Virden, J. W.; Tarasevich, B. J.; Chick, L. A. *Adv. Colloid Interface Sci.* **1996**, 69, 131. (f) Crooks, R. M.; Ricco, A. J. *Acc. Chem. Res.* **1998**, 31, 219.
- (2) (a) Liu, G.-Y.; Xu, S.; Qian, Y. *Acc. Chem. Res.* **2000**, 33, 457. (b) Xia, Y.; Whitesides, G. M. *Angew. Chem., Int. Ed. Engl.* **1998**, 37, 550. (c) Gorman, C. B.; Carroll, R. L.; He, Y.; Tian, F.; Fuierer, R. *Langmuir* **2000**, 16, 6312. (d) Bumm, L. A.; Arnold, J. J.; Charles, L. F.; Dunbar, T. D.; Allara, D. L.; Weiss, P. S. *J. Am. Chem. Soc.* **1999**, 121, 8017. (e) Weiss, P. S.; Yokota, H.; Aebersold, R.; van den Engh, G.; Bumm, L. A.; Arnold, J. J.; Dunbar, T. D.; Allara, D. L. *J. Phys.: Condens. Matter* **1998**, 10, 7703. (f) Hobara, D.; Sasaki, T.; Imabayashi, S.-i.; Kakiuchi, T. *Langmuir* **1999**, 15, 5073. (g) Piner, R. D.; Zhu, J.; Xu, F.; Hong, S.; Mirkin, C. A. *Science* **1999**, 283, 661. (h) Hong, S.; Mirkin, C. A. *Science* **2000**, 288, 1808. (i) Hong, S.; Zhu, J.; Mirkin, C. A. *Science* **1999**, 286, 523. (j) Chen, J.; Reed, M. A.; Asplund, C. L.; Cassell, A. M.; Myrick, M. L.; Rawlett, A. M.; Tour, J. M.; Van Patten, P. G. *Appl. Phys. Lett.* **1999**, 75, 624.
- (3) (a) Stranick, S. J.; Parikh, A. N.; Tao, Y.-T.; Allara, D. L.; Weiss, P. S. *J. Phys. Chem.* **1994**, 98, 7636. (b) Stranick, S. J.; Atre, S. V.; Parikh, A. N.; Wood, M. C.; Allara, D. L.; Winograd, N.; Weiss, P. S. *Nanotechnology* **1996**, 7, 438. (c) Stranick, S. J.; Kamna, M. M.; Krom, K. R.; Parikh, A. N.; Allara, D. L.; Weiss, P. S. *J. Vac. Sci. Technol. B* **1994**, 12, 2004.
- (4) *n*-Decanethiol was used as received from Lancaster Synthesis, Windham, NH. The gold substrates were purchased from Molecular Imaging, Inc., Phoenix, AZ.
- (5) Clegg, R. S.; Hutchison, J. E. *J. Am. Chem. Soc.* **1999**, 121, 5319.
- (6) Poirier, G. E. *Chem. Rev.* **1997**, 97, 1117.
- (7) Bumm, L. A.; Arnold, J. J.; Dunbar, T. D.; Allara, D. L.; Weiss, P. S. *J. Phys. Chem. B* **1999**, 103, 8122.
- (8) Stranick, S. J.; Parikh, A. N.; Allara, D. L.; Weiss, P. S. *J. Phys. Chem.* **1994**, 98, 11136.
- (9) Bumm, L. A.; Arnold, J. J.; Cygan, M. T.; Dunbar, T. D.; Burgin, T. P.; Jones, L., II; Allara, D. L.; Tour, J. M.; Weiss, P. S. *Science* **1996**, 271, 1705.
- (10) Klotz, I. M.; Farnham, S. B. *Biochemistry* **1968**, 7, 3879 and references therein.
- (11) (a) The van der Waals interaction energy of a methylene group with its neighbors within a SAM in a vacuum is derived from the heat of sublimation (ΔH_{sub}) of *n*-alkanes versus chain length (taken from NIST database: <http://webbook.nist.gov>). Plotting ΔH_{sub} of *n*-alkanes as a function of *n*-alkane chain length yields a slope whose value is the van der Waals interaction energy per methylene unit. An estimate for the stabilization due to individual van der Waals interactions of the methylene matrix is 8.6 kJ/mol $-\text{CH}_2-$. While these values are referenced to gas phase, they do provide a reasonable estimate for the relative energetic values of this system. (b) The interaction energies in a series of *N*-methylenamides of the formula $\text{C}_n\text{H}_{2n+1}\text{CONHCH}_3$ ($n = 9, 11, 13, 15$) were reported in Davies, M.; Jones, A. H. *Trans. Faraday Soc.* **1959**, 55, 1329.
- (12) (a) Clegg, R. S.; Hutchison, J. E. *Langmuir* **1996**, 12, 5239. (b) Clegg, R. S.; Reed, S. M.; Smith, R. K.; Barron, B. L.; Rear, J. A.; Hutchison, J. E. *Langmuir* **1999**, 15, 8876.